Post-steam-treatment of Mo/HZSM-5 Catalysts: An Alternative and Effective Approach for Enhancing Their Catalytic Performances of Methane Dehydroaromatization

Hongxia Wang, Lingling Su, Jianqin Zhuang, Dali Tan, Yide Xu,* and Xinhe Bao*

State Key Laboratory of Catalysis, Dalian Institute of Chemical Physics, The Chinese Academy of Sciences, 457 Zhongshan Road, P.O. Box 110, Dalian 116023, China

Received: December 13, 2002; In Final Form: September 15, 2003

Post-steam-treatment is a facile and effective method for improving the catalytic performances of Mo/HZSM-5 catalysts in methane dehydroaromatization under nonoxidative conditions. The treatment can enhance the stability of the catalyst and also give a higher methane conversion and a higher yield of light aromatics, as well as a decrease in the formation rate of carbonaceous deposits. ^{27}Al, ^{29}Si, and ^{1}H multinuclear magic angle spinning nuclear magnetic resonance, X-ray photoelectron spectroscopy, X-ray diffraction, X-ray fluorescence spectroscopy, and thermogravimetric analysis measurements as well as catalytic reaction evaluations were employed to conduct comparative studies on the properties of the catalysts before and after the post-steam-treatment. The results revealed that the number of free Brönsted acid sites per unit cell decreased, while more Mo species migrated into the HZSM-5 channels for the 6Mo/HZSM-5 catalysts after the post-steam-treatment. In addition, the average pore diameter was also larger for the post-steam-treated catalysts, and this was advantageous for mass transport of the reaction products. However, a severe post-steam-treatment, i.e., with longer treating time, of the 6Mo/HZSM-5 catalyst will lead to the formation of the $Al_2(MoO_4)_3$ phases, which is detrimental to the reaction.

1. Introduction

The direct conversion of methane to valuable chemicals is a great challenge to catalytic chemists. Recently, the methane dehydroaromatization (MDA) reaction over Mo/HZSM-5 catalysts under non-oxidative conditions has received great attention.[1−3] After about 10 years of research around the world on the MDA reaction at 973 K over Mo/HZSM-5 catalysts, it is now a common recognition that the MDA reaction is quite complicated. However, the following points are generally accepted. First, Mo/HZSM-5 is a bifunctional catalyst. Second, there exists an induction period during which the molybdenum oxide species are reduced by CH_4 and transformed into molybdenum carbides and/or oxycarbides, and these carbidic species are the active sites responsible for methane activation and for the formation of unsaturated C_2 species. Third, the unsaturated C_2 species thus formed will oligomerize into light aromatics over the Brönsted acid sites. And last, due to the fact that the reaction is carried out at 973 K without using oxidants, carbonaceous deposits are formed severely via various reaction pathways such as the direct pyrolysis of methane into carbon and hydrogen and/or the severe condensation reaction of unsaturated C_2 species. The MDA reaction pathway can be expressed as follows:

(1) $CH_4 \leftrightarrows CH_x$ ($x \leq 3$) $\leftrightarrows C_2H_y$ ($y \leq 4$) $\leftrightarrows$ light aromatics (mainly C_6H_6) $\leftrightarrows$ polyaromatics, accompanied by the formation of H_2 at each stage;

(2) $CH_4 \leftrightarrows C + H_2$, accompanied by severe condensation reactions of unsaturated C_2 species to form polyaromatic-like carbonaceous deposits.

Up to now, Mo/HZSM-5 has been regarded as the best catalyst among all the tested catalysts. However, heavy formation of carbonaceous deposits renders serious obstacles for further understanding of this reaction and putting it into commercial applications.

In the case of a solid acid, such as HZSM-5 zeolite, no matter whether it is used as a catalyst or as a catalyst component, coke formation is closely related to the nature and distribution of the acid sites.[4−6] Therefore, many investigations have aimed at solving this problem via adjusting and controlling the distribution of the acid sites. Lin and co-workers[7] reported that significant improvement could be achieved on a Mo catalyst supported on HZSM-5 pre-dealuminated via steam treatment for 6 h. The C_6H_6 yield increased by 32%, while the selectivity to coke dropped dramatically from 20 to 8%, as compared with the un-pretreated Mo/HZSM-5 catalyst under similar catalytic reaction conditions. Further studies on this catalyst led to the conclusion that only a small fraction of the Brönsted acid sites was required to accomplish the aromatization.[8] Iglesia and co-workers[9] claimed that selective silanation of the external acid sites on HZSM-5 by means of large organosilane molecules could decrease the content of the acid sites as well as the number of the MoO_x species retained at the external surface. On samples prepared using a silica-modified HZSM-5 zeolite, MoO_x precursors and active MoC_x species that were formed during the CH_4 reaction at 950 K were found to reside predominantly inside the zeolite channels. Accordingly, the spatial constraints so imposed could inhibit the bimolecular chain-growth pathways. As a result, the hydrocarbon formation rates on a 4% Mo/silica-modified HZSM-5 (4Mo/Si-HZSM-5) increased by about 30%, while the deactivation rates decreased, as compared with those on a 4Mo/HZSM-5 catalyst. These results clearly demonstrated that the Mo species migrating into and residing in the zeolite channels are more effective for the MDA reaction. Ichikawa and co-workers[10] have reported that dealumination of the HMCM-22 zeolite by acid reflux with an aqueous solution of

* Corresponding authors. Fax: 0086-411-4694447. E-mails: xhbao@dicp.ac.cn; xuyd@dicp.ac.cn.

10.1021/jp0225931 CCC: $25.00
Published on Web 11/01/2003

6 M HNO_3 at 373 K for 10 h resulted in an effective suppression of the strong Brönsted acid sites, thus greatly enhancing the catalytic performance for MDA over the dealuminated Mo/HMCM-22 catalyst. Anyway, it is common to adjust and control the distribution of the acid sites of the corresponding zeolites for the present preparation methods of MDA catalysts, which is usually carried out before the Mo impregnation and calcination stages.

By using the ^{1}H MAS NMR technique, we have recently demonstrated that the driving force for the Mo species to move into the HZSM-5 zeolite channels and the interaction between the Mo species and the Brönsted acid sites on the Mo/HZSM-5 catalysts are closely related to the number of Brönsted acid sites per unit cell.[3,11] Therefore, the dealumination of HZSM-5 or HMCM-22 zeolites, which leads to a decrease in the number of strong Brönsted acid sites, may diminish the driving force for the migration of Mo species into the channels and decrease the amount of Mo species residing in the zeolite channels.

These results stimulated us to speculate that a post-steam-treatment procedure for the Mo/HZSM-5 catalysts, i.e., steam-treating the Mo/HZSM-5 catalysts after the impregnation of Mo on the HZSM-5 zeolite and the calcination of the catalysts, might be an alternative approach for suppressing the superfluous Brönsted acid sites and for increasing the stability of the catalysts. Moreover, it is well-known that steam-treating is advantageous for dispersing transition metal oxides on the surface of metal oxide supports to form the monolayer dispersion state.[12] This is also valid for zeolite catalyst systems modified by transition metal ions.[13,14] Thus, it is expected that a post-steam-treatment to the Mo/HZSM-5 catalyst would further promote the migration of the Mo species into the channels.

Recently, we have investigated the effect of post-steam-treatment of the Mo/HZSM-5 catalysts on their catalytic performances in the MDA reaction. The results demonstrate that post-steam-treatment of the Mo/HZSM-5 catalysts is also an effective procedure for enhancing their activities and stabilities. These improvements mainly come from a proper suppression of the excess number of Brönsted acid sites per unit cell and from a better distribution of the Mo species in the zeolite channels. In this study, we report on our findings obtained by using techniques of multinuclear magic angle spinning nuclear magnetic resonance (MAS NMR), X-ray photoelectron spectroscopy (XPS), X-ray diffraction (XRD), and X-ray fluorescence spectroscopy (XRF), as well as by catalytic evaluation. These studies can help us to understand the effect of the post-steam-treatment on the Mo/HZSM-5 catalysts and the behavior of the treated catalysts in comparison with the untreated ones.

2. Experimental Section

(2.1) Catalyst Preparation. The parent Mo/HZSM-5 catalyst was prepared by the conventional impregnation method with a similar procedure as previously described in ref 15. The HZSM-5 zeolite with a Si/Al ratio of 25 was supplied by Nankai University (Tianjin, China). It was impregnated with an aqueous solution of ammonium heptamolybdate for 24 h at room temperature. Then it was dried for 3 h at 393 K, followed by calcination in static air at 773 K for 4 h. The Mo/HZSM-5 catalysts were hereafter denoted as *x*Mo/HZSM-5, where *x* is the Mo content in weight percent. The 6Mo/HZSM-5 catalyst thus prepared was further treated at 813 K in flowing steam (mixed with Ar, with $Ar/H_2O = 2.33$ in molar ratio); then 6Mo/HZSM-5(STAI-*t*) catalysts were obtained. Here, "AI" means after impregnation of the Mo species with HZSM-5 and calcination, and the "*t*" represents the time of steam treatment (ST) in hours.

(2.2) Catalysts Evaluation. The evaluation of the catalysts with the MDA reaction was carried out in a quartz tubular fixed-bed reactor under atmospheric pressure at 973 K, and the catalyst charge was 0.5 g. It was first heated under a He stream to 973 K and maintained at this temperature for 30 min. After the pretreatment, the reactant gas was introduced into the reactor at a space velocity of 1500 mL/(g·h). The tail gas was regularly and automatically sampled and analyzed by a Varian 3800 online gas chromatograph. It was equipped with a flame ionization detector (FID) for the analysis of hydrocarbons such as CH_4, C_6H_6, C_7H_8, and $C_{10}H_8$, etc., and a thermal conductivity detector (TCD) for the analysis of H_2, N_2, CH_4, CO, C_2H_4, and C_2H_6. About 10% N_2 in the feed gas was used as an internal standard for the analysis of all products, including deposited coke, as suggested by Lunsford and co-workers.[16,17] The reaction results were expressed as methane conversions, while the yields of the products and the selectivities toward the products such as C_6H_6, C_7H_8, and $C_{10}H_8$, etc., were calculated on the basis of the consumed methane molecules.

(2.3) Catalysts Characterization. *(2.3.1) BET, XRD, and SEM.* Specific surface areas and average pore diameters of the samples were obtained by the BET method at liquid nitrogen temperature of 78 K, using a value of 0.162 nm^2 for the cross-sectional area of N_2. The measurements were performed with Micromeritics ASAP-2000 equipment, and the data were processed and analyzed by an IBM computer.

XRD patterns were obtained on a Rigaku diffractometer using Cu Kα radiation at room temperature, with instrumental settings of 40 kV and 50 mA. Powder diffractograms of the samples were recorded over a set of 2*q* values ranging from 5 to 50° at a scanning rate of 5°/min. All XRD patterns were recorded, stored, and processed by a computer system. The relative crystallinities of the 6Mo/HZSM-5 and 6Mo/HZSM-5(STAI-*t*) catalysts were quantified by comparing the intensities of the strongest peaks at an angle of 23.1° (2θ) with that of HZSM-5 zeolite, while the intensity of the characteristic peak of HZSM-5 is assumed to be 100%.

The scanning electron microscopy (SEM) pictures of the samples were taken on an HB-600 microscope with an accelerating voltage of 25 kV, on which the images of the catalysts were obtained with the same magnification of 5000.

(2.3.2) XRF, XPS, and TGA. The actual Mo content in weight percent and the bulk Si/Al ratio of each catalyst were analyzed by the XRF technique. XRF experiments were performed on a Philips MagiX X-ray fluorescence spectrometer, and IQ+ standardless quantitative software was employed for analysis.

The Mo contents and the amounts of carbonaceous deposits in the near-surface regions of the used catalysts were determined by the XPS technique. The XPS spectra were recorded on a modified Leybold LHS 12 MCD system using Al Kα radiation with a power of 300 W and a pass energy of 100 eV. The binding energies reported in this work were calibrated using Si(2p) as the internal standard (BE = 103 eV). The ratio of atoms and the near-surface compositions of the samples were calculated from peak areas and corresponding peak area sensitivity factors, based on the empirical data of ref 18, which was taken from the appendix of the handbook of X-ray photoelectron spectroscopy published by the Perkin-Elmer Corp. Each sample was pressed into a tablet at room temperature and placed on a sample bracket, which was made of tantalum; after being evacuated at 10^{-9} Torr in the pretreatment chamber the sample was transferred into the analysis chamber for XPS measurement.

Thermal gravimetric analysis (TGA) was performed on a Perkin-Elmer TGS-2 thermogravimetric apparatus. A 30 mg amount of the coked catalyst was used when the sample was heated from room temperature to 973 K at a heating rate of 10 K/min in an air stream with a flow rate of 30 mL/min.

(2.3.3) ^{27}Al, ^{29}Si, and ^{1}H MAS NMR. ^{27}Al, ^{29}Si, and ^{1}H MAS NMR experiments were carried out on a Bruker DRX-400 spectrometer with a BBO MAS probe using a 4 mm ZrO_2 rotor. The deconvolution of the spectra was conducted using the Bruker software. The ^{27}Al MAS NMR spectra were recorded at 104.3 MHz using a 0.75 μs (π/12) pulse and with 1024 scans. A 1% $Al(NO_3)_3$ aqueous solution was used as the reference of chemical shifts. The ^{29}Si MAS NMR spectra were recorded at 79.5 MHz using a 0.8 μs (π/4) pulse with 1024 scans, and the chemical shifts were referenced to 4,4-dimethylsilapentane sulfonate sodium (DSS). The framework Si/Al ratio of the HZSM-5 zeolite was determined according to the equation given in ref 19:

$$\mathrm{Si/Al} = [\sum_{n=0}^{4} I_{\mathrm{Si}(n\mathrm{Al})}]/\sum_{n=0}^{4} \frac{1}{4} n I_{\mathrm{Si}(n\mathrm{Al})}]$$

where the $I_{\mathrm{Si}(n\mathrm{Al})}$ is the intensity of the individual Si(nAl) peaks (% area) obtained from the corresponding deconvoluted spectra. Prior to the ^{1}H MAS NMR experiment, the samples were dehydrated at 673 K for 20 h in a homemade apparatus. All the ^{1}H MAS NMR spectra were recorded at 400.1 MHz using a 1 μs (π/10) pulse with 100 scans. The chemical shifts were referenced to a saturated aqueous solution of DSS. The quantitative results for the numbers of hydroxyl groups in different environments per unit cell were obtained from the corresponding deconvoluted ^{1}H MAS NMR spectra. The number of Brönsted acid sites per unit cell in the parent HZSM-5 was determined on the basis of the number of framework Al ions per unit cell in the parent HZSM-5, which was calculated from the framework Si/Al ratio together with the chemical composition formula of HZSM-5 zeolite. Moreover, the number of Brönsted acid sites thus obtained equals to the sum of B1 sites and B2 sites. Then the number of B1 sites per unit cell in Mo/HZSM-5 and Mo/HZSM-5(STAI-t) samples were estimated by comparing their special peak areas with that in the parent HZSM-5 zeolite. But for other hydroxyl groups, such as silanol (1.7 ppm) and nonframework Al−OH (2.2 ppm) as well as the small amount of water residues in the channels (4.9 ppm), the numbers were calculated by comparing the peak areas concerned with that of B1 in the same deconvoluted ^{1}H MAS NMR spectrum. All the caclulations for the number of different hydroxyl groups are based on each sample having the same content of HZSM-5.

3. Results

(3.1) XRF, BET, XRD, and SEM. The Mo contents and the bulk Si/Al ratios of the samples measured by the XRF technique are listed in Table 1. The average Mo content of all five samples is (5.22 ± 0.14)%. It seems that the loss of the Mo content of the catalysts does not occur after the post-steam-treatment under the given conditions. The atomic Si/Al ratio of the bulk for all samples obtained by the XRF measurements also remained constant (22.9 ± 0.5). Therefore, it is clear that there were no changes in chemical compositions in the bulk of the 6Mo/HZSM-5 catalysts after the post-steam-treatments under the given experimental conditions.

The physical properties of the 6Mo/HZSM-5 and 6Mo/HZSM-5(STAI-t) catalysts obtained from BET measurements are also listed in Table 1. The BET data of the samples demonstrate that there was a gradual decrease in surface area from 298 to 277 m^2/g and an increase in the average pore diameter from 1.48 to 1.64 nm for the 6Mo/HZSM-5 and 6Mo/HZSM-5(STAI-3h) samples and that the changes mentioned above occurred primarily in the first 0.5−1 h of treatment, which suggests that the hydrothermal treatment caused a slight increase in the average pore diameter. The XRD patterns of all samples are shown in Figure 1. The XRD peaks, which are characteristic of the crystallite phases HZSM-5 zeolite, remained almost the same. The average relative crystallinity of the 6Mo/HZSM-5 and 6Mo/HZSM-5(STAI-t) catalysts was (77.6 ± 3.9)%, suggesting that the relative crystallinity of all samples measured by XRD did not change very much with increasing post-steaming time (see Table 1). However, the corresponding SEM images shown in Figure 2 illustrate that there was a slight change in the morphology of the crystallites. The crystallites of the parent 6Mo/HZSM-5 were in a more perfect state than that of the fresh 6Mo/HZSM-5(STAI-3h). Some damage existed on the edge of the crystallites in the latter case.

TABLE 1: Properties of HZSM-5, 6Mo/HZSM-5, and Corresponding STAI-*t* Samples

sample	surface area[a] (m^2/g)	av pore diam[a] (nm)	Mo loading[b] (%)	Si/Al ratio in bulk[b]	rel crystallinity[c] (%)
HZSM-5	348.8	1.51			100
6Mo/HZSM-5	298.1	1.48	5.33	23.1	79.4
STAI-0.5h	284.5	1.54	5.28	23.4	77.4
STAI-1h	277.5	1.63	5.12	22.5	80.7
STAI-2h	282.8	1.63	5.28	22.7	73.7
STAI-3h	277.5	1.64	5.08	22.9	76.8

[a] From BET characterization. [b] From XRF characterization. [c] From XRD characterization.

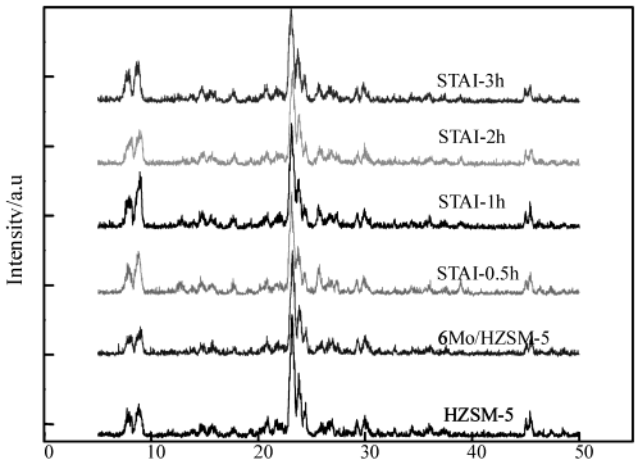

Figure 1. XRD patterns of HZSM-5, 6Mo/HZSM-5, and 6Mo/HZSM-5(STAI-t) samples.

(3.2) XPS and TGA. The valence states of the Mo species and the near-surface chemical compositions of both the 6Mo/HZSM-5 and 6Mo/HZSM-5(STAI-0.5h) samples were studied by using the XPS technique. As shown in Figure 3, the Mo species, existing in both the fresh 6Mo/HZSM-5(STAI-0.5h) and 6Mo/HZSM-5 catalysts, are mainly in the Mo^{6+} state, as evidenced by the fact that the measured binding energies of the doublet centers at 232.1 and 235.3 eV, which is in good agreement with the results reported by other authors.[16,21−23] In addition, there is a small peak at the lower binding energy of 227 eV, forming another doublet with the peak at the higher energy of 239.1 eV, which can be assigned to the tantalum.

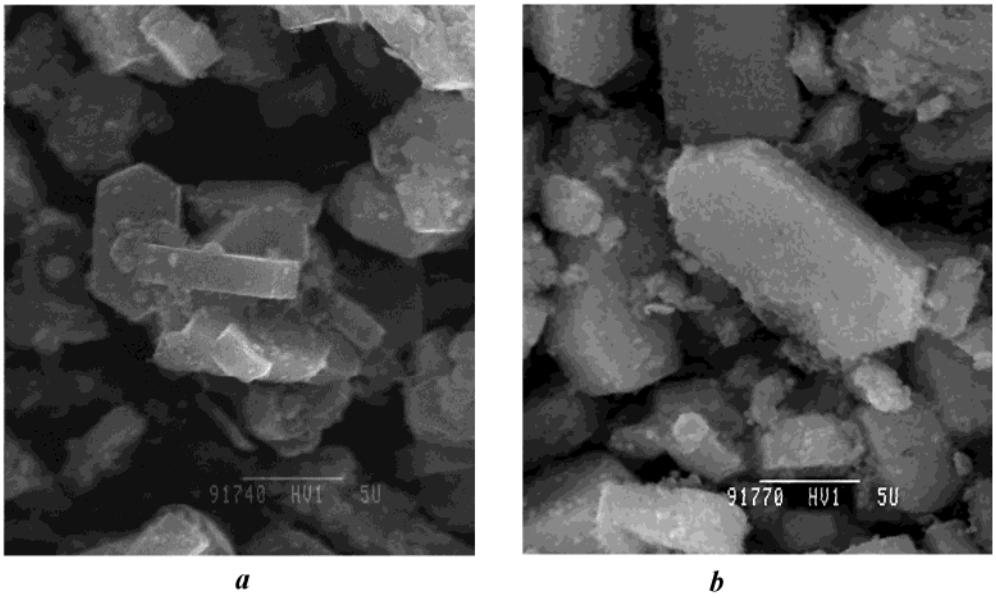

Figure 2. SEM images of fresh (a) 6Mo/HZSM-5 and (b) 6Mo/HZSM-5(STAI-3h) samples.

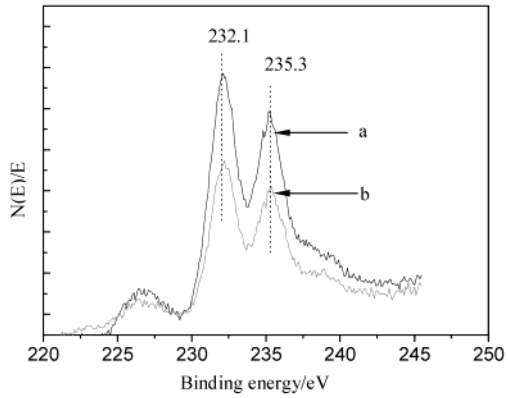

Figure 3. XPS spectra in Mo 3d region recorded from fresh (a) 6Mo/HZSM-5 and (b) 6Mo/HZSM-5(STAI-0.5h) catalysts.

TABLE 2: Near-Surface Chemical Compositions (%) and Mo/Si Ratios of Fresh (a) 6Mo/HZSM-5 and (b) Corresponding STAI-*t* Samples Determined by XPS

	composition (%)				
sample	Mo 3d	O 1s	Si 2p	C 1s	Mo/Si
6Mo/HZSM-5	4.0	66.0	14.9	15.1	0.27
STAI-0.5h	2.6	62.5	17.3	17.6	0.15
STAI-1h	3.2	57.9	17.5	21.3	0.18
STAI-2h	2.8	67.1	15.3	16.1	0.18
STAI-3h	3.3	56.9	18.8	20.9	0.17

The Mo 3d region in the fresh 6Mo/HZSM-5 XPS spectra is similar to that in the freshly steam-treated 6Mo/HZSM-5(STAI-0.5h) catalyst, and this indicates that the post-steam-treatment to 6Mo/HZSM-5 catalyst could not cause a change in the chemical state of the Mo species under the given experimental conditions. The Mo 3d region of the XPS spectra also suggested that there was a certain amount of Mo species locating on the external surface of both the 6Mo/HZSM-5 and 6Mo/HZSM-5(STAI-0.5h) catalysts. Furthermore, the relative concentrations of the various constituents of all the samples in the near-surface region are listed in Table 2. Here, the difference caused by Ta 4d is assumed to be negligible due to the insignificant change in the Ta 4d signal relative to the strong difference in intensity of Mo 3d signal. The Mo/Si ratio of the 6Mo/HZSM-5 catalyst in the near-surface region decreased from 0.27 to 0.15 when it was treated by steam for 0.5 h, and then it remained at 0.18 when the steaming time was increased from 1 to 3 h.

Figure 4 shows the XPS spectra of the C 1s and Si 2p regions of the 6Mo/HZSM-5 and 6Mo/HZSM-5(STAI-0.5h) catalysts after running the MDA reaction for 10 h. The decrease in the amount of carbonaceous species in the near-surface region is obvious. The C/Si atomic ratio declines from 2.34 on the coked 6Mo/HZSM-5 catalyst to 1.51 on the coked 6Mo/HZSM-5(STAI-0.5h) catalyst; i.e., the carbonaceous deposits in the near surface region of the used 6Mo/HZSM-5(STAI-0.5h) catalyst decreased to ca. 65% of those on the used 6Mo/HZSM-5 catalyst. This implies that the post-steam-treatment is advantageous for the 6Mo/HZSM-5 catalysts in suppressing the formation of carbonaceous species.

In addition to the XPS measurements of near-surface carbonaceous species on the 6Mo/HZSM-5 and 6Mo/HZSM-5(STAI-0.5h) catalysts, which had been used in the reaction for 10 h, the TGA technique was also employed to study the suppression of the total carbonaceous deposits on the 6Mo/HZSM-5(STAI-0.5h) catalyst. Figure 5 presents the d*G*/d*T* profiles of both the coked 6Mo/HZSM-5 catalyst and the coked 6Mo/HZSM-5(STAI-0.5h) catalyst. The corresponding areas of the two profiles decreased obviously. If we take the area under the profile as a measure of the total amount of carbonaceous deposits on/in the catalyst, the amount of coke on the 6Mo/HZSM-5(STAI-0.5h) catalyst decreased to about 45% of that on the 6Mo/HZSM-5 catalyst. Again, it demonstrated that the carbonaceous species formed during the MDA reaction are significantly suppressed on the 6Mo/HZSM-5(STAI-0.5h) catalyst, as compared with the untreated 6Mo/HZSM-5 catalyst.

(3.3) Multinuclear MAS NMR. *(3.3.1) ^{27}Al MAS NMR.* The ^{27}Al MAS NMR spectra of the 6Mo/HZSM-5 and 6Mo/HZSM-5(STAI-*t*) samples were studied to elucidate the change in coordination environment of different Al species as well as the interaction between the Mo species and the framework Al after the post-steam-treatment. Generally, two peaks were detected in each ^{27}Al MAS NMR spectrum (see Figure 6). One is at ca. $\delta = 52$, which is typically associated with the four-coordinated framework Al in HZSM-5 zeolite, and the other centers at about $\delta = -0.8$, which can be assigned to the six-coordinated extraframework Al species.[24] By increasing the time of post-steam-treatment, the intensity of the framework Al species in

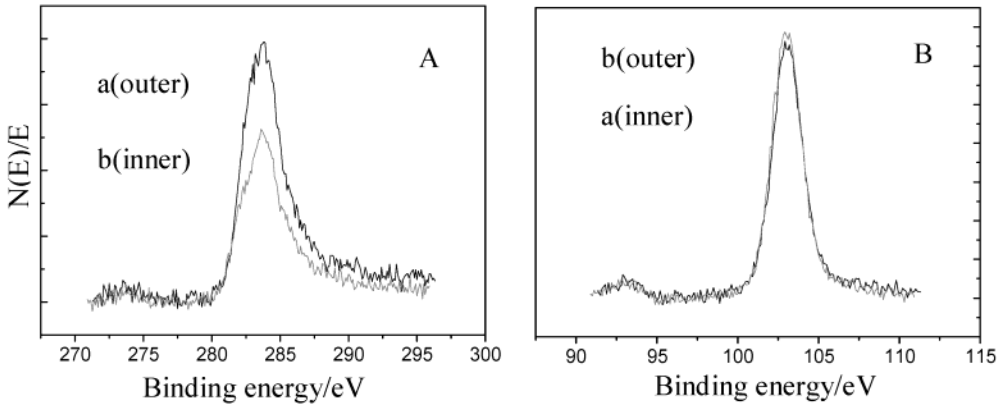

Figure 4. XPS spectra in the (A) C 1s region and (B) Si 2p region for spent (a) 6Mo/HZSM-5 and (b) 6Mo/HZSM-5(STAI-0.5h) catalysts with 10 h of reaction time.

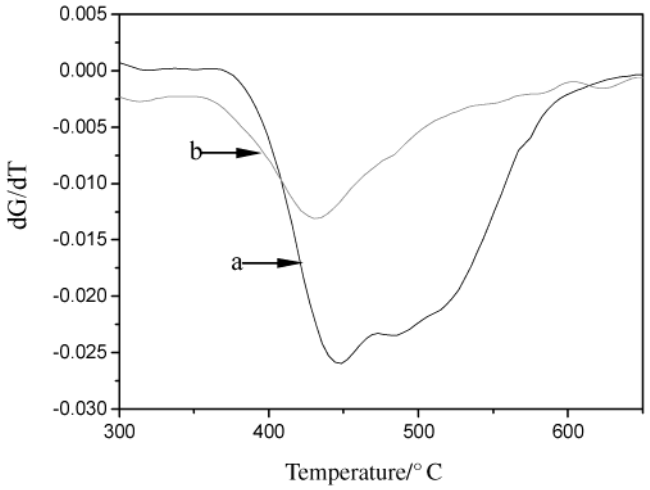

Figure 5. The d*G*/d*T* profile of used catalysts with 10 h of running time: (a) 6Mo/HZSM-5 sample; (b) 6Mo/HZSM-5(STAI-0.5h) sample.

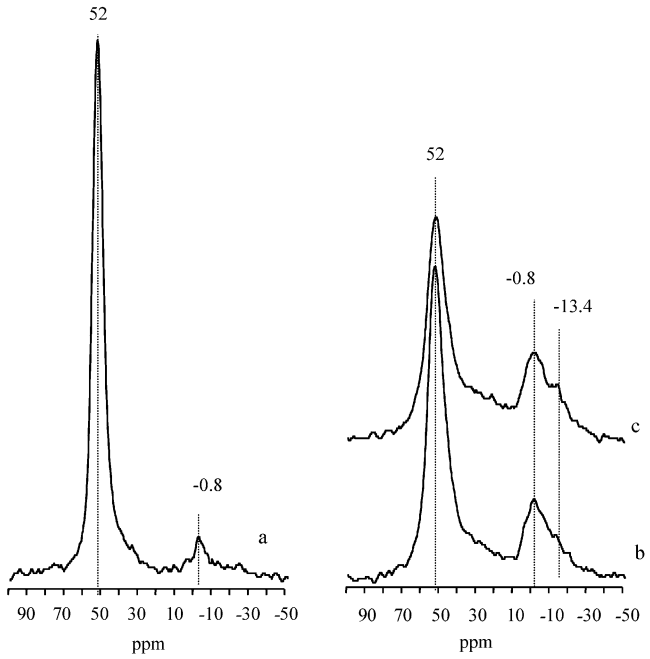

Figure 6. ^{27}Al MAS NMR spectra of (a) 6Mo/HZSM-5, (b) 6Mo/HZSM-5(STAI-0.5h), and (c) 6Mo/HZSM-5(STAI-3h) catalysts.

the 6Mo/HZSM-5(STAI-*t*) sample decreased, which was accompanied by an increase in the intensity of the nonframework Al species. A new peak as a shoulder of the −0.8 ppm peak

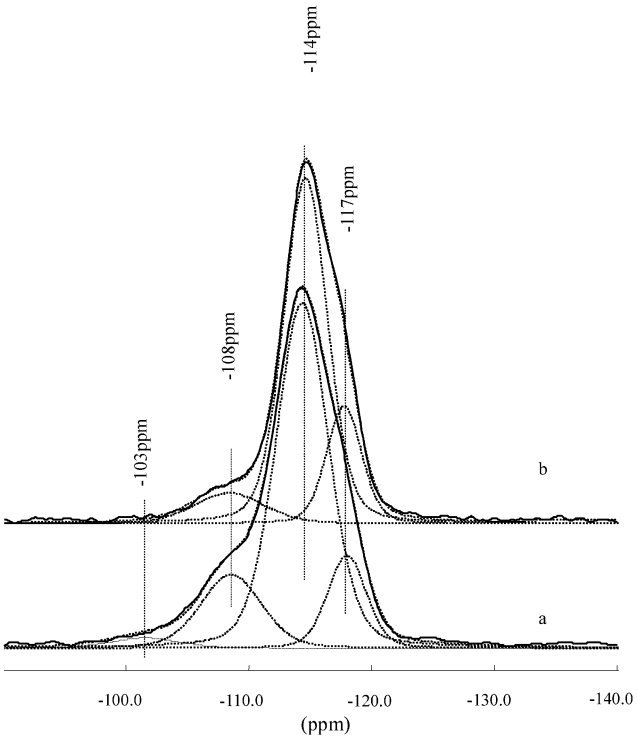

Figure 7. ^{29}Si MAS NMR spectra of (a) 6Mo/HZSM-5 and (b) 6Mo/HZSM-5(STAI-0.5h) catalysts.

appeared at ca. $\delta = -13.4$, which is attributed to octahedral aluminum in the form of crystallite $Al_2(MoO_4)_3$.[24,25] A study of the transformation between the framework and nonframework Al species indicates that dealumination occurred under the hydrothermal treatment condition. The longer the post-steaming time, the more nonframework Al species are formed. In addition, the $Al_2(MoO_4)_3$ crystallites, which are thought to be an inactive species for MDA,[26,27] are also formed gradually.

(3.3.2) ^{29}Si MAS NMR. The ^{29}Si MAS NMR spectra of the samples and their deconvolution curves are shown in Figure 7. Four peaks can be observed in the ^{29}Si MAS NMR spectra on the 6Mo/HZSM-5 and 6Mo/HZSM-5(STAI-*t*) catalysts after deconvoluting them by Gaussian and Lorentzian line shapes. The first peak at ca. $\delta = -103$ is due to the sites of Si(OH)-$(OSi)_3$ groups.[26,28] It almost disappeared on the 6Mo/HZSM-5(STAI-0.5h) catalyst, as can be seen from Figure 7. The second peak at ca. $\delta = -108$ is generally attributed to the silicons having one Al atom as the neighbor and is designated as Si-(1Al), while the third peak at ca. $\delta = -114$ stems from the

TABLE 3: Si/Al Ratios Calculated from the ^{29}Si MAS NMR Spectra of 6Mo/HZSM-5 and Corresponding STAI-*t* Samples

sample	Si(*n*Al)	δ (ppm)	fwhm (Hz)	*I* (% area)	Si/Al
6Mo/HZSM-5	Si(1Al)	−108.5	5.8	16.5	24.2
	Si(0Al)	−114.3	5.1	67.6	
	Si(0Al)	−117.9	3.7	13.4	
	silanol	−101.5	6.6	2.5	
STAI-0.5h	Si(1Al)	−108.4	6.7	9.9	40.4
	Si(0Al)	−114.6	4.2	70.7	
	Si(0Al)	−117.7	3.4	19.4	
STAI-1h	Si(1Al)	−108.4	6.7	7.9	50.9
	Si(0Al)	−114.7	4.2	75.2	
	Si(0Al)	−117.7	3.4	16.9	
STAI-2h	Si(1Al)	−108.4	6.8	7.2	55.5
	Si(0Al)	−114.9	4.5	80.7	
	Si(0Al)	−118.1	3.5	12.1	
STAI-3h	Si(1Al)	−108.4	6.5	5.8	68.7
	Si(0Al)	−114.8	4.2	77.9	
	Si(0Al)	−117.9	3.3	16.3	

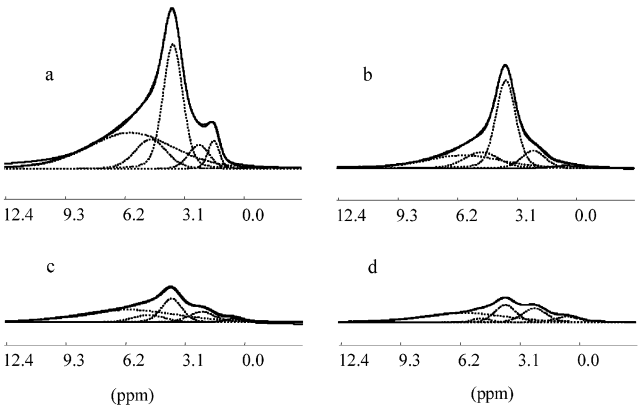

Figure 8. ^{1}H MAS NMR spectra of samples (a) HZSM-5, (b) 6Mo/HZSM-5, (c) 6Mo/HZSM-5(STAI-0.5h), and (d) 6Mo/HZSM(STAI-3h).

silicons having no Al atoms as the neighbor, i.e., the Si(0Al) groups. The fourth peak at ca. $\delta = -117$ is commonly attributed to the crystallographically inequivalent sites of Si(0Al) groups.[29]

The deconvolution results and the Si/Al ratio in the framework thus calculated are listed in Table 3. The Si/Al ratio in the framework of the 6Mo/HZSM-5 was ca. 24.2. It increased with the time of post-steam-treatment increasing and reached ca. 68.7 for the 6Mo/HZSM-5(STAI-3h) sample. The results confirm that framework Al species were indeed extracted with the post-steam-treatment of the 6Mo/HZSM-5 catalysts. The longer the post-steaming time, the more framework Al species are extracted. As the Si/Al ratio in the bulk remained unchanged, the extracted framework Al species should reside on the external surface or in the channels, and in the form of alumina crystallites or $Al_2(MoO_4)_3$ crystallites.

(3.3.3) ^{1}H MAS NMR. The ^{1}H MAS NMR spectra of the samples are shown in Figure 8. Five different bands could be identified on each sample on the basis of deconvolution according to the Gaussian and Lorentzian shapes. The first band centering at $\delta = 3.7$, denoted as B1, is generally ascribed to free bridging hydroxyl groups locating at the intersections of the HZSM-5 zeolites.[30] The second band at ca. $\delta = 4.9$ is attributed to the H_2O adspecies residual in the channels of the HZSM-5 zeolites.[31] The third band at the lower field of $\delta = 5.9$, denoted as B2, is assigned to disturbed or restricted bridging OH groups, which are influenced by an electrostatic interaction from the zeolite framework.[30] In addition, two types of hydroxyl groups associated with framework Si and nonframework Al were also detected in the ^{1}H MAS NMR spectra of the HZSM-5 and the 6Mo/HZSM-5 samples. One of the hydroxyl groups with a chemical shift at ca. $\delta = 2.2$ is typically attributed to Al−OH groups, in which the hydroxyl protons form hydrogen bonds via anchoring to neighboring framework oxygen atoms.[30,32,33] Another hydroxyl group pertaining to the band at around $\delta = 1.7$ is assigned to $Si(OH)(OSi)_3$, i.e., the silanol groups. In consistency with the ^{29}Si MAS NMR spectra, the band at around $\delta = 1.7$ was almost undetectable on the post-steam-treated samples. But a new band at ca. $\delta = 0.5$ had developed on 6Mo/HZSM-5(STAI-*t*) samples, which can be attributed to the undisturbed Al−OH in the channels or at the outer surface of the HZSM-5 zeolite.[30]

The quantitative results for the number of hydroxyl groups in different environments per unit cell are listed in Table 4. The suppression of the free Brönsted acid sites per unit cell is evident after the 6Mo/HZSM-5 catalysts were treated by steam. The number of free Brönsted acid sites per unit cell, i.e., B1, decreased obviously from 1.3 of the untreated 6Mo/HZSM-5 catalyst to 0.3 of the 6Mo/HZSM-5(STAI-3h) sample. However, the number of B2 sites per unit cell seemed to change little with the increase in the post-steaming time.

(3.4) Catalyst Evaluation and the Role of the Post-steam-treatment. The catalytic performances of the MDA over the untreated 6Mo/HZSM-5 and the 6Mo/HZSM-5(STAI-*t*) catalysts after running the reaction for 60 and 420 min are listed in Table 5. It can be seen that not only the methane conversion and the BTX (benzene, toluene, and xylene, but mainly benzene) yield increased over the post-steam-treated catalyst, as compared with those on the untreated 6Mo/HZSM-5 catalysts, but also the formation rates of benzene and toluene increased over the 6Mo/HZSM-5(STAI-*t*) catalysts. Among these samples, the 6Mo/HZSM-5(STAI-0.5h) catalyst shows the best performance, with a BTX yield of 8.1% at an on-stream time of 60 min and 6.5% at an on-stream time of 420 min. The formation rate of light aromatics had an increase of ca. 30% on the 6Mo/HZSM-5(STAI-0.5h), in comparison with that of the 6Mo/HZSM-5 catalyst.

Figure 9 shows the plots of methane conversion and the BTX yield on 6Mo/HZSM-5 and 6Mo/HZSM-5(STAI-0.5h) vs time on stream. Remarkable improvement in the catalytic performance was observed over the 6Mo/HZSM-5(STAI-0.5h) cata-

TABLE 4: Number of Different Hydroxyls per Unit Cell Estimated from ^{1}H MAS NMR Spectra of HZSM-5, 6Mo/HZSM-5, and Corresponding STAI-*t* Samples

	no. of hydroxyls/(unit cell)					
sample	3.7 ppm (B1)	5.9 ppm (B2)	4.9 ppm (water)	2.2 ppm (Al-OH[a])	1.7 ppm (Si-OH)	0.5 ppm (Al-OH[a])
HZSM-5	1.8	2.2	0.6	0.4	0.2	-
6Mo/HZSM-5	1.3	0.7	0.4	0.3	0.05	-
STAI-0.5h	0.7	0.6	0.1	0.1		0.1
STAI-1h	0.4	0.3	0.1	0.4		0.2
STAI-2h	0.4	0.6	0.1	0.2		0.1
STAI-3h	0.3	0.6	0.1	0.2		0.1

[a] Two types of extraframework Al−OH.

TABLE 5: Comparison of Catalytic Behaviors between 6Mo/HZSM-5 and Corresponding STAI-*t* Samples after Running the Reaction for 60 and 420 min, Respectively[a]

			formation rate of products, (nmol/(g·s))				
sample (run time (min))	CH_4 conv (%)	BTX[b] yields (%)	C_2	C_6	C_7	C_{10}	coke select (%)
6Mo/HZSM-5 (60)	11.5	6.3	-	1110	59.5	316	27.1
STAI-0.5h (60)	13.6	8.1	61.4	1427	72.5	387	22.8
STAI-1h (60)	13.1	7.4	65.1	1302	70.7	337	26.8
STAI-2h (60)	12.1	7.3	42.8	1295	72.5	290	24.3
STAI-3h (60)	12.1	6.9	20.5	1218	68.8	283	29.4
6Mo/HZSM-5 (420)	5.6	3.7	128.3	630.6	47.6	60.3	16.5
STAI-0.5h (420)	9.6	6.5	106.0	1134	78.1	126.5	19.6
STAI-1h (420)	8.6	5.7	113.5	985.8	70.7	104.2	20.0
STAI-2h (420)	8.2	5.2	87.4	900.2	67.0	85.6	24.8
STAI-3h (360)[c]	8.0	5.1	111.6	887.2	66.2	89.6	22.3

[a] Reaction condition: 973 K with a SV of 1500 mL/(g·h). [b] BTX: the abbreviation of benzene, toluene, and xylene. [c] Data were taken after running the reaction for 360 min.

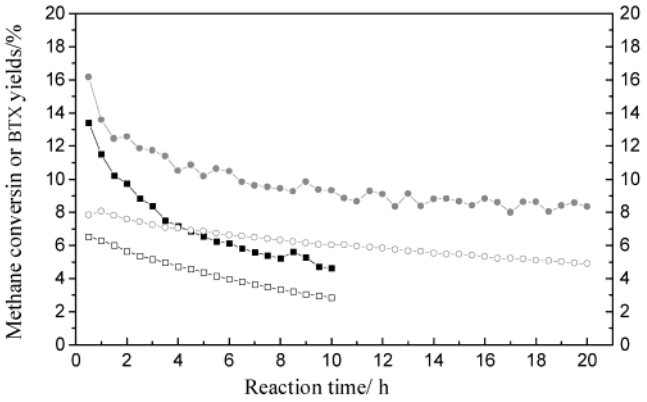

Figure 9. Catalytic performance of 6Mo/HZSM-5 (■,□) and 6Mo/HZSM-5(STAI-0.5h) (●,○) catalysts: solid symbols for CH_4 conversion, and open symbols for BTX yields. The reaction runs at 973 K with a space velocity of 1500 mL/(g·h).

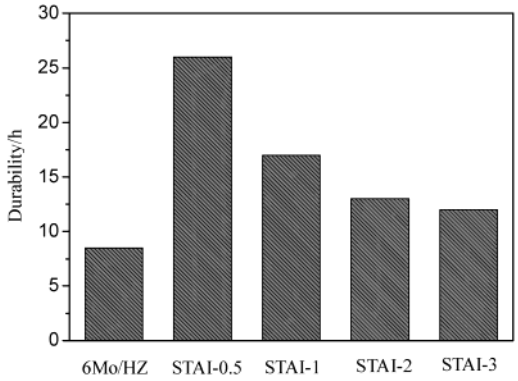

Figure 10. Durability of 6Mo/HZSM-5 and 6Mo/HZSM-5(STAI-*t*) catalysts, taking it as a criterion to stop the reaction when the initial BTX yield on each catalyst dropped to its half-value.

lyst. Not only the methane conversion and the BTX yield increased, but also the catalytic stability was greatly improved. On the 6Mo/HZSM-5(STAI-0.5h) catalyst, after running for 20 h, the BTX yield was about 5% at a methane conversion of ca. 8.3%, whereas, on the 6Mo/HZSM-5 catalyst after running only for 10 h, the BTX yield dropped to ca. 2.8% at a methane conversion of ca. 4.6%.

The effect of post-steaming time of the 6Mo/HZSM-5 catalysts on their catalytic performances was also investigated. Figure 10 demonstrates that the catalytic performances of the 6Mo/HZSM-5 catalysts were very sensitive to the time of post-steaming. With an increase of the post-steaming time from 0.5 to 3 h, all of the 6Mo/HZSM-5(STAI-*t*) samples exhibited a longer lifetime than that of the parent 6Mo/HZSM-5. The durability of the 6Mo/HZSM-5(STAI-*t*) catalysts, however, decreased gradually with the increasing of post-steaming time. Apparently, the durability of the 6Mo/HZSM-5(STAI-0.5h) catalyst was approximately three times longer than that of the 6Mo/HZSM-5 catalyst, if we take half of initial BTX yield of each sample as a criterion for terminating the reaction.

4. Discussion

It is well-known that dealumination will occur if the HZSM-5 zeolite is treated by steam,[8,34−36] and the treatment will also cause a reduction in the number of Brönsted acidic sites per unit cell. However, in our present case, when the 6Mo/HZSM-5 catalyst was treated by steam, the situation is quite complicated. First, the Si/Al ratio in the framework, as measured by the ^{29}Si MAS NMR technique, increased with increasing of the time of post-steam-treatment. Thus, the number of free Brönsted acid sites, B1, would decrease, as revealed by the ^{1}H MAS NMR results. Accordingly, the number of free Brönsted acid sites per unit cell was obviously suppressed to ca. 50% on the 6Mo/HZSM-5(STAI-0.5h) sample, as compared with that of the untreated 6Mo/HZSM-5 catalyst. Surprisingly, such suppression of the free Brönsted acid sites per unit cell on the 6Mo/HZSM-5(STAI-0.5h) resulted in a more active and stable catalyst for MDA. A possible explanation is that only a small amount of the free Brönsted acid sites per unit cell is necessary to accomplish the aromatization reaction after the intermediates are formed on the catalyst surface. Therefore, the present study on the post-steam-treatment of the Mo/HZSM-5 catalysts in this point is consistent with the conclusion that has been put forward by us in ref 8.

Second, the XPS measurement shows that the Mo/Si ratio in the near-surface region of the 6Mo/HZSM-5 catalyst decreased from 0.27 to 0.15 when it was treated by steam for 0.5 h, and then remained at 0.18 when the steaming time was increased from 1 to 3 h. One reason that might account for the decrease in the Mo/Si ratio in the near-surface region of the 6Mo/HZSM-5(STAI-*t*) catalysts is the growth of the Mo-containing crystallites. Evidence for growth of the Mo-containing crystallites and accompanying decrease in their dispersion was not found in the XRD patterns of the 6Mo/HZSM-5 and 6Mo/HZSM-5(STAI-*t*) catalysts. Also, the explanation for the growth of the Mo-containing crystallites is contradictory with the above-mentioned results of catalytic evaluation over the 6Mo/HZSM-5 and 6Mo/HZSM-5(STAI-*t*) catalysts since larger MoO_x crystallite precursors are unfavorable for the MDA reaction. Therefore, a decrease in the Mo/Si ratio in the near-surface region due to the growth of the Mo crystallites can be ruled out. It is reasonable to conclude that part of the Mo species at

the external surface migrated into the channels of the HZSM-5 zeolite after the 6Mo/HZSM-5 catalysts were treated by steam in view of the fact that the bulk concentration of the Mo species in all samples were similar, as illustrated in the XRF results.

The Mo species originally located on the external surface of the zeolite migrated into and resided in the channels during the post-steam-treatment, as evidenced by the behavior of the XPS Mo/Si ratios. Knozinger and co-workers[12] reported the monolayer dispersion in physical mixtures of MoO_3 and Al_2O_3, particularly in the presence of water vapor, in the temperature range of 723−823 K. Fierro and co-workers[13] reported the migration of Mo species into intracrystalline cavities in ammonium heptamolybdate-impregnated Na−Y zeolite. They found that in the presence of water vapor, even with very low water vapor pressure, the impregnated precursors of MoO_3 crystallites located on the external surface would volatilize with the formation of $MoO_2(OH)_2$, which more easily migrates into the zeolite and results in a redistribution of the Mo species. Iglesia and co-workers[27,37] have also prepared the Mo/HZSM-5 catalysts with most of Mo species in the channels of HZSM-5 zeolite by a solid-state reaction method and studied the location and change of the Mo species during the preparation process in greater detail. They found that the MoO_x species migrated onto the external surface first at ca. 623 K. Then, at temperatures between 773 and 973 K, the MoO_x species migrated into the zeolite channels via surface movement and gas-phase transport, exchanged at the acid sites, and reacted to form H_2O. Therefore, in the present work Mo species migrating into and residing in the channels by means of the interaction between the Mo species and the Brönsted acidic sites during the post-steam-treatment will also make a contribution to the suppression of the superfluous Brönsted acidic sites in the channels. $MoO_2(OH)_2$ species formed in the presence of water vapor have a larger molecular size. It appears that the $MoO_2(OH)_2$ species are much easier to interact with the free Brönsted acid sites than to interact with the restricted Brönsted acid sites as we can see from Table 4. Further work on this issue now is underway in our Group.

The Mo species in the channels as precursors of the active sites for the MDA are more active and stable than those on the external surface of the zeolite, as demonstrated by Iglesia and co-workers.[9,38] Our present study demonstrates that more Mo species migrated into the channels of zeolite by post-steam-treatment and also confirms that the Mo species in the channels are more active and stable than the Mo species on the external surface for the MDA reaction. On the other hand, the formation of the $Al_2(MoO_4)_3$ phases, due to the strong interaction between the Mo species and the framework Al, will result in a loss of both the Mo species in the channels and the number of free Brönsted acid sites, B1 to a certain degree. This will in turn lead to a decrease in the catalytic stability of the 6Mo/HZSM-5 catalyst treated by steam for a relatively long time, as in the case for the 6Mo/HZSM-5(STAI-3h) catalyst.

The suppression of carbonaceous species on the outer surface of the 6Mo/HZSM-5(STAI-0.5h) catalysts is probably due to the existence of less molybdenum species on the external surface, as compared with that of the 6Mo/HZSM-5 catalysts (see the section on XPS characterization). On the other hand, the decrease in the number of the Brönsted acid sites caused by the exchange of molybdenum species with Brönsted acid sites and the dealumination resulting from post-steam-treatment also make a contribution to the suppression of the carbonaceous species on the Brönsted acid sites. This is reflected in the TGA results. It can be easily seen that there are more than one type of carbonaceous species on coked 6Mo/HZSM-5 and 6Mo/HZSM-5(STAI-0.5h) catalysts. And the coke deposits formed on the 6Mo/HZSM-5 catalyst were suppressed greatly after the catalyst was treated by steam for 0.5 h. Therefore, the procedure of post-steam-treatment for the 6Mo/HZSM-5(STAI-0.5h) catalyst exhibited a remarkable advantage for suppressing coke deposition, as compared with the untreated 6Mo/HZSM-5 catalyst.

Last, it is well-known that steam treatment of the HZSM-5 zeolite can cause a change of its morphology. This is also true for the post-steam-treatment of the 6Mo/HZSM-5 catalysts. Typically, the average pore diameter increased from 1.48 to 1.64 nm after the post-steam-treatment. The mass transport involved in the MDA reaction certainly will be benefited from such increase in pore diameters. This kind of physical properties is important when considering the difference in molecule size between the reactant and the products and is worthy of further studies.

5. Conclusions

(1) Post-steam-treatment of the Mo/HZSM-5 catalysts is an effective way to enhance their catalytic activity and stability for the MDA reaction. The effect of this treatment on the chemical composition of the bulk and the relative crystallinity is negligible.

(2) Mild post-steam-treatment can lead to a proper decrease in the number of free Brönsted acid sites and a compatible increase of the Mo species in the channels. As a result, coke formation on the Brönsted acid sites as well as on the Mo species are both suppressed, resulting in a remarkable enhancement of the catalytic stability of the 6Mo/HZSM-5(STAI-0.5h) catalyst.

(3) Severe post-steam-treatment will lead to the formation of the $Al_2(MoO_4)_3$ species, which will cause a loss of the Mo species in the channels and a heavy extraction of framework Al, and thus be detrimental to the MDA reaction.

(4) Steaming treatment to the 6Mo/HZSM-5 catalysts can cause a certain change of its morphology, particularly, the average pore diameter will increase with the time of post-steam-treatment. In this way, the mass transport in the MDA reaction probably becomes easier.

Acknowledgment. Financial supports from the Ministry of Science and Technology of China, the Natural Science Foundation of China, the Chinese Academy of Sciences, and the BP-China Joint Research Center are gratefully acknowledged.

References and Notes

(1) Xu, Y.; Lin, L. *Appl. Catal., A* **1999**, *188*, 53.
(2) Shu, Y.; Ichikawa, M. *Catal. Today* **2001**, *71*, 55.
(3) Xu, Y.; Bao, X. H.; Lin, L. W. *J. Catal.* **2003**, *216*, 386.
(4) Bibby, D. M.; Millestone, N. B.; Patterson, J. E.; Aldridge, L. P. *J. Catal*. **1986**, *97*, 493.
(5) Guisnet, M.; Magnoux, P. *Stud. Surf. Sci. Catal*. **1994**, *88*, 53.
(6) Sahoo, S. K.; Viswanadham, N.; Ray, N.; Gupta, J. K.; Singh, I. D. *Appl. Catal., A* **2001**, *205*, 1.
(7) Lu, Y.; Ma, D.; Xu, Z.; Tian, Z.; Bao, X.; Lin, L. *Chem. Commun*. **2001**, *20*, 2048.
(8) Ma, D.; Lu, Y.; Su, L.; Xu, Z.; Tian, Z.; Xu, Y.; Lin, L.; Bao, X. *J. Phys. Chem. B* **2002**, *106*, 8524.
(9) Ding, W.; Meitzner, G. D.; Iglesia, E. *J. Catal*. **2002**, *206*, 14.
(10) Shu, Y.; Ohnishi, R.; Ichikawa, M. *Catal. Lett*. **2002**, *81*, 9.
(11) Su, L.; Yan, Z.; Liu, X.; Xu, Y.; Bao, X. *J. Nat. Gas Chem*. **2002**, *11*, 18.
(12) Leyrer, J.; Zaki, M. I.; Knozinger, H. *J. Phys. Chem*. **1986**, *90*, 4775.
(13) Fierro, J. L. G.; Conesa, J. C.; Agudo, A. L. *J. Catal*. **1987**, *108*, 334.
(14) Huang, M.; Yao, J.; Xu, S.; Meng, C. *Zeolites* **1992**, *12*, 810.
(15) Ma, D.; Shu, Y.; Bao. X.; Xu, Y. *J. Catal*. **2000**, *189*, 314.

(16) Wang, D.; Lunsford, J. H.; Rosynek, M. P. *Top. Catal*. **1996**, *3*, 289.
(17) Wang, D.; Lunsford, J. H.; Rosynek, M. P. *J. Catal*. **1997**, *169*, 347.
(18) Wagner, C. D.; Davis, L. E.; Zeller, M. V.; Taylor, J. A.; Raymond, R. M.; Gale, L. H. *Surf. Interface Anal*. **1981**, *3*, 211.
(19) Fyfe, C. A.; Gobbi, G. C.; Kennedy, G. J.; Graham, J. D.; Ozubku, R. S.; Murphy, W. J.; Bothner-By, A.; Dadok, J.; Chesnick, A. S. *Zeolites* **1985**, *5*, 179.
(20) Shu, J.; Adnot, A.; Grandjean, B. P. *Ind. Eng. Chem. Res*. **1999**, *38*, 3860.
(21) DeVries, J. E.; Yao, H. C.; Baird, R. J.; Gandhi, H. S. *J. Catal*. **1983**, *84*, 8.
(22) Dai, P. E.; Lunsford, J. H. *J. Catal*. **1980**, *64*, 173.
(23) Yang, T.; Lunsford, J. H. *J. Catal*. **1987**, *103*, 55.
(24) Liu, W.; Xu, Y.; Wong, S.; Wang, L.; Qin, J.; Yang, N. *J. Mol. Catal. A: Chem.* **1997**, *120*, 257.
(25) Zhang, J. Z.; Long, M. A.; Howe, R. F. *Catal. Today* **1998**, *44*, 293.
(26) Zhang, W. P.; Ma, D.; Han, X. W.; Liu, X. M.; Bao, X. H. *J. Catal*. **1999**, *188*, 393.
(27) Kim, Y. H.; Borry, R. W., III; Iglesia, E. *Microporous Mesoporous Mater*. **2000**, *495*, 35.
(28) Zhang, W.; Bao, X.; Guo, X.; Wang, X. *Catal. Lett*. **1999**, *60*, 89.
(29) Brunner, E.; Ernst, H.; Freude, D.; Frohlich, T.; Hunger, M.; Pfeifer, H. *J. Catal*. **1991**, *127*, 34.
(30) Hunger, M. *Catal. Rev.−Sci. Eng*. **1997**, *39* (4), 345.
(31) Hunger, M.; Freude, D.; Pfeifer, H. *J. Chem. Soc., Faraday Trans*. **1991**, *87*, 657.
(32) Lohse, U.; Löffler, E.; Hunger, M.; Stöckner, J.; Patzelová, V. *Zeolites* **1987**, *7*, 11.
(33) Brunner, E.; Ernst, H.; Freude, D.; Froehlich, T.; Hunger, M.; Pfeifer, H. *Stud. Surf. Sci. Catal*. **1989**, *49*, 623.
(34) Zholobenko, V. L.; Kustov, L. M.; Kazansky, V. B.; Loeffler, E.; Lohser, U.; Peuker, Ch.; Oehlmann, G. *Zeolites* **1990**, *10*, 304.
(35) Datka, J.; Marschmeyer, S.; Neubauer, T.; Meusinger, J.; Papp, H.; Schütze, F.-W.; Szpyt, I. *J. Phys. Chem*. **1996**, *100*, 14451.
(36) Triantafillidis, C. S.; Vlessidis, A. G.; Nalbandian, L.; Evmiridis, N. P. *Microporous Mesoporous Mater*. **2001**, *47*, 369.
(37) Borry, R. W., III; Kim, Y. H.; Huffsmith, A.; Reimer, J. A.; Iglesia, E. *J. Phys. Chem. B* **1999**, *103*, 5787.
(38) Li, W.; Meitzner, G. D.; Borry, R. W., III; Iglesia, E. *J. Catal*. **2000**, *191*, 373.